ARTICLES SCIENCE CHINA Materials

mater.scichina.com link.springer.com

Published online 19 October 2016 | doi: 10.1007/s40843-016-5128-0
Sci China Mater 2016, 59(10): 842–850

SPECIAL ISSUE: Excitonic Solar Cells (II)

Enhancement of photovoltaic performance by two-step dissolution processed photoactive blend in polymer solar cells

Rong Hu[1†], Jiang Cheng[1†], Haitao Ni[1], Jiang Zhu[1], Hongdong Liu[1], Wei Zhang[2*], Yurong Liu[1], Lu Li[1], Chaozhong Guo[1*] and Kaibo Zheng[2,3*]

ABSTRACT **We reported enhanced performance of polymer solar cells, based on poly(3-hexylthiophene):[6,6]-phenyl-C_{61}-butyric acid methyl ester (P3HT:$PC_{61}BM$) and poly-thieno[3,4-b]-thiophene-*co*-benzodithiophene:[6,6]-phenyl-C_{71}-butyric acid methyl ester (PTB7:$PC_{71}BM$) photovoltaic systems, by a two-step dissolution treatment of photoactive blends. Optical and morphological characterization revealed that the composition of the ordered polymer and donor/acceptor phase structure in the photoactive layer can be optimized using a two-step dissolution treatment. In addition, time-resolved photoluminescence indicated that exciton dissociation efficiency could be increased using this method. Current density-voltage (*J-V*) measurements showed that power conversion efficiencies (PCE) of the two-step dissolution treated devices were higher than those of one-step treated devices by 24% and 8% for P3HT:$PC_{61}BM$ and PTB7:$PC_{71}BM$ systems, respectively. Therefore, this two-step dissolution treatment further optimizes the performance of polymer solar cells.**

Keywords: polymer solar cells, photoactive layer, two-step dissolution, power conversion efficiency

INTRODUCTION

Polymer solar cells (PSCs) have attracted wide attention owing to their valuable features, such as low-cost, lightweight, flexible, and the possibility of widespread manufacturing [1–4]. Recently, a series of studies showed that power conversion efficiency (PCE) of PSCs can be greatly improved by utilizing novel highly efficient donor (D) and acceptor (A) materials and optimizing the interface structure regulation and design of the device [5–9]. However, the state of art efficiency of PSCs is still lower than 15%, which is far from the commercialization standard [10]. Hence, further improvement is needed to realize the practical application of PSCs.

The morphology and structure of the photoactive layer in PSCs have great influence on the photo-physical process and the performance of the devices [11–14]. The morphology of the photoactive layer can be optimized towards better uniformity, crystallinity, and enhanced D/A interface area by engineering the solution process of the PSCs [15–18], which includes the selection of a proper solvent with high solubility of the polymer [19,20], using mixed solvent systems [21–23], and combining the additive and solvent [24]. Besides the above methods, approaches like solution heating [25], solution freeze-drying [26], and the poor solvent inducing method [27] have also been used to regulate the morphology and structure of the photoactive layer. Recently, we found that polymers undergo self-aggregation even in the solution-phase, which strongly depends on the solvents. Such a self-aggregated conformation of polymers can inhabit the photo-induced charge generation process in PSCs [28–30]. Therefore, regulating such self-aggregation by adjusting the dissolution processes of polymers is expected to enhance the device performance of PSCs. Hereby, we developed a new two-step dissolution process to fabricate

[1] Research Institute for New Materials Technology, Chongqing University of arts and sciences, Chongqing 402160, China
[2] Division of Chemical Physics, Lund University, Lund 221 00, Sweden
[3] Gas Processing Center, College of Engineering, Qatar University, PO Box 2713, Doha, Qatar
[†] These authors contributed equally to this work.
[*] Corresponding authors (emails: wei.zhang@chemphys.lu.se (Zhang W); guochaozhong1987@163.com (Guo C); kaibo.zheng@chemphys.lu.se (Zheng K))

poly(3-hexylthiophene):[6,6]-phenyl-C61-butyric acid methyl ester (P3HT:PC61BM) and polythieno[3,4-b]-thiophene-co-benzodithiophene:[6,6]-phenyl-C71-butyric acid methyl ester (PTB7:PC71BM) solar cells. This method can effectively enhance the PCE of the devices, which can be attributed to the improvement of the morphology. Based on a time-resolved photoluminescence (PL) study, we can further confirm more efficient exciton dissociation in the two-step processed P3HT compared with the one-step processed counterparts. This two-step dissolution treatment further optimizes the performance of polymer solar cells.

EXPERIMENTAL SECTION

Preparation of solution

P3HT, PTB7, $PC_{61}BM$ and $PC_{71}BM$ were purchased from Lumtec. Fig. 1 shows their chemical structures. In order to prepare the P3HT:$PC_{61}BM$ mixed solution, P3HT:$PC_{61}BM$ (1:1, wt., 20 mg mL^{-1}) was first dissolved in the initial solvent chloroform (CF) and stirred for 12 h at room temperature (25°C). The mixed solution was then exposed to the air until the CF solvent completely volatilize. Afterwards, the dried P3HT:$PC_{61}BM$ mixture was redissolved in the second solvent *o*-dichlorobenzene (*o*-DCB) as the precursor solution for fabrication of the photoactive layer. The mixed solution of PTB7:$PC_{71}BM$ was prepared using a similar method with different concentration in initial CF solution (PTB7 10 mg mL^{-1}, $PC_{71}BM$ 15 mg mL^{-1}) and a different second solvent (chlorobenzene:1,8-diiodooctane=97%:3%, by volume).

Fabrication and characterization of polymer solar cells

The structure of the PSCs consists of indium tin oxide (ITO) glass, zinc oxide (ZnO), photoactive layer, molybdenum oxide (MoO_3), and an Ag electrode. The ITO glass substrate (1.5×1.5 cm^2) was cleaned using ultrasonication in detergent and was successively washed with deionized water, acetone, ethanol, and isopropyl alcohol. After that, a 60 μL ZnO precursor solution (zinc acetate:2-methoxyethanol:ethanolamine = 10 g : 10 mL: 0.28 mL) was spin-coated (3000 rpm, 30 s) on the ITO glass, followed by annealing for 60 min on the heating plate (200°C). A blend of the photoactive mixed solution was then spin-coated on the ZnO film in an argon-purged glovebox (oxygen concentration < 0.1 ppm). The spin coating parameters of P3HT:$PC_{61}BM$ were 1000 rpm for 20 s. The following solvent vapor annealing (SVA) was performed under *o*-DCB atmosphere for 12 h. Alternatively, the parameters of PTB7:$PC_{71}BM$ were 850 rpm for 50 s. Finally, a 5 nm MoO_3 layer and 50 nm Ag electrode were successively evaporated on the top of the blend.

The current density-voltage (*J*-*V*) measurement of the PSCs was carried out by a Keithley 2400 source meter. A xenon light source was used to give an irradiance of 100 mW cm^{-2} (equivalent to AM 1.5) at the surface of the PSCs. The external quantum efficiency (EQE) was measured in the air at room temperature by a solar cell spectral response measurement system (SOFN Instruments Co. Ltd.). The surface morphology of the photoactive layer was characterized by an atomic force microscope in tapping mode (AFM, Dimension Edge). The absorption spectrum of the photoactive layer was measured using a UV-visible spectrophotometer with a wavelength range of 300–700 nm (Hitachi U-3900).

Time resolved photoluminescence (TRPL) characterization

A Ti:sapphire laser (Spectra-Physics, Tsunami) at 800 nm and a repetition rate of 81 MHz with a pulse duration of 100 fs was used as an excitation source. Frequency-doubled light (400 nm, generated by Photop Technologies, Tripler TP-2000B) was used for excitation. PL was collected by using two 1 in. quartz plano-convex lenses (50 mm focal length) focused on the input slit of a spectrograph (Chromex). The output of the spectra was sent to the streak camera (Hamamatsu C6860) with a slit width of 20

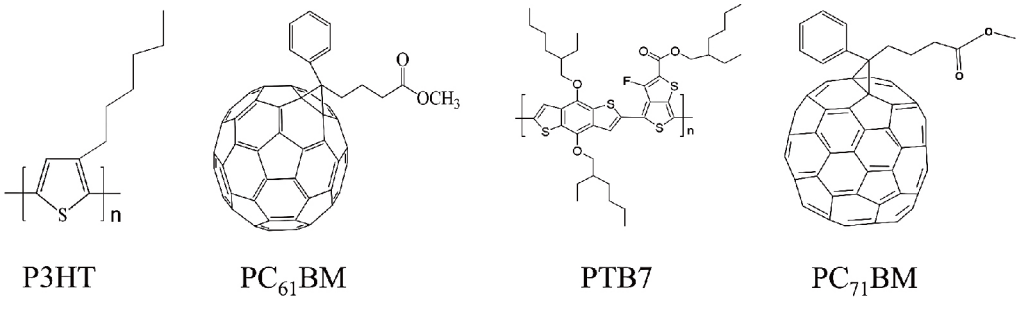

Figure 1 Chemical structures of P3HT, $PC_{61}BM$, PTB7 and $PC_{71}BM$.

μm. After background correction of the measured PL images, shading and spectral sensitivity correction of the fluorescence spectra was performed using a calibrated reference light source (Ocean Optics, LS-1-CAL). All samples were kept in N_2 atmosphere and measured at room temperature. Efforts were taken to keep the alignment of the experimental set-ups the same for all the samples.

RESULTS AND DISCUSSION

P3HT has been regarded as a classic hole transporting material with good solubility and self-organizing capability. In addition, bulk heterojunction (BHJ) P3HT:$PC_{61}BM$ solar cells have good reproducibility of photovoltaic device performance. Hence, we use a P3HT:$PC_{61}BM$ system to explore the effect of the two-step dissolution process on the performance of the device. Table 1 lists the preparation parameters of four solution processes for comparison in this study.

Steady-state absorption spectra of the photoactive layer

The optical absorption properties of P3HT:$PC_{61}BM$ blend films are shown in Fig. 2. The absorption of $PC_{61}BM$ is assigned in the ultraviolet region, while the P3HT mainly absorbs light within the visible region. For Device 1, the absorption band of P3HT ranges from 350 to 650 nm with a maximum absorption peak at 480 nm. In addition, a weak shoulder peak occurs at 600 nm; this shoulder peak can be attributed to the 0'-0 vibration transition originating from the ordered phase of P3HT [12,31]. After the P3HT:$PC_{61}BM$ was treated by the two-step dissolution process (Device 3), the absorption spectrum was red-shifted with a more pronounced shoulder peak at 600 nm compared with the one-step treated device (Device 1). This indicates that more P3HT ordered phase is formed in the photoactive layer via the two-step dissolution process. We also noticed that after the post-treatment by SVA, the 600 nm peak of the two-step process increases compared with that of the one-step process. This suggests that the two-step dissolution process can modulate the phase structure of P3HT.

Morphological Characterization

The morphologies of the blend films in four P3HT:$PC_{61}BM$ devices were investigated via AFM. As can be seen in Fig. 3, the dissolution process and post-treatment can affect the morphology of the photoactive layer. In Device 1, the surface morphology of the photoactive layer is rather smooth with a root-mean-square (RMS) roughness of 0.70 nm, suggesting relatively poor D/A phase separation [32]. When treated with the two-step dissolution process, the surface morphology of the photoactive layer becomes rougher (RMS=0.99 nm, Device 3), suggesting the improvement of P3HT ordered aggregation [33]. After the SVA post-treatment, significant changes in the morphology of the photoactive layers are observed. The AFM image of the photoactive layer in Device 2 exhibits a significantly fluctuating morphology and coarse phase structure, with RMS=4.42 nm. This trend is inconsistent with previous literature [34]. On the other hand, the RMS of the photoactive layer of Device 4 is further increased to 6.02 nm. This indicates that the morphology of the photoactive layer can be optimized both via the two-step dissolution process and SVA post-treatment.

Photovoltaic behaviors of P3HT:$PC_{61}BM$ devices

Fig. 4a shows the *J-V* characteristics of four P3HT:$PC_{61}BM$ devices, with their respective parameters summarized in Table 2. The detailed performance of devices can be found in Supplementary information (Fig. S1). As shown in Fig. 4, strong influence of photoactive layer morphology on device performance (short circuit current density (J_{sc}), open circuit voltage (V_{oc}), fill factor (FF) and PCE) can be observed. After the two-step dissolution process, the J_{sc} of Device 3 is obviously improved from 5.16 mA cm^{-2} to 6.10 mA cm^{-2} compared with that of Device 1. In SVA-treated devices, enhancement of J_{sc} by the two-step dissolution process is also observed (10.71 mA cm^{-2} in Device 4 compared with 10.03 mA cm^{-2} in Device 2). Such enhancement in J_{sc} can be attributed to the ordered P3HT phase and the increased interface area according to the optical absorption and morphology characterization of

Table 1 Preparation methods of photoactive layer for P3HT:$PC_{61}BM$ photovoltaic devices

Samples	Solvent 1	Treatment	Solvent 2	Spin-coating	Post-treatment
Device 1	-	-	*o*-DCB	1000 rpm, 20 s	Fast dry
Device 2	-	-	*o*-DCB	1000 rpm, 20 s	SVA[b)]
Device 3	CF	SV[a)]	*o*-DCB	1000 rpm, 20 s	Fast dry
Device 4	CF	SV[a)]	*o*-DCB	1000 rpm, 20 s	SVA[b)]

a) Solvent volatilization; b) solvent vapor annealing.

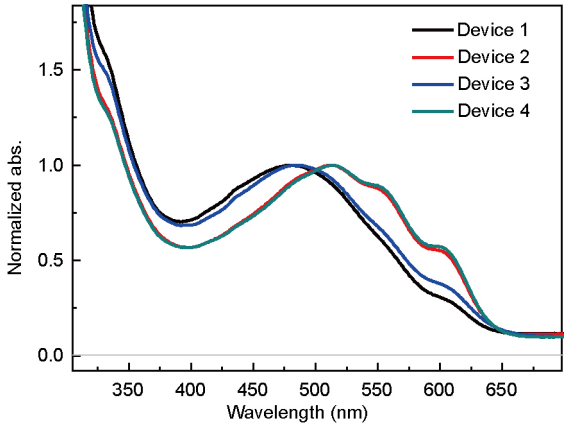

Figure 2 Normalized absorption spectra of P3HT:$PC_{61}BM$ photoactive layers with varies preparation conditions depicted in Table 1.

photoactive layers (see Figs 2 and 3). In addition, we can observe a slight decrease of V_{oc} by 2 to 14 mV for devices treated with the dissolution process, as seen in Table 2. The V_{oc} of the device was determined by the highest occupied molecular orbital (HOMO) energy level of the donor and the lowest unoccupied molecular orbital (LUMO) energy level of the acceptor [35]. According to Tsio's study [36], the HOMO energy level of P3HT can be greatly modified by its morphology and structure. Therefore, we can conclude the slight decrease of V_{oc} is induced by a slight elevation of the HOMO level in the P3HT ordered phase by the two-step solution process. Moreover, slight improvement of the FF is noticed for the two-step treated Devices 2 and 4. Consequently, the highest PCE among all four devices, 3.93% is obtained in Device 4.

As shown in Table 2, the J_{sc} of the devices is most sensitive to the dissolution process and SVA post-treatment. In order to analyze the mechanism of increasing photocurrent, we measured the EQE of P3HT:$PC_{61}BM$ devices with different fabrication processes, as shown in Fig. 4b. Substantial increases of the EQE within the entire absorption region can be observed for both the two-step dissolution process and SVA post-treatment of the photoactive layers. The maximum EQE values of Device 1, Device 2, Device 3,

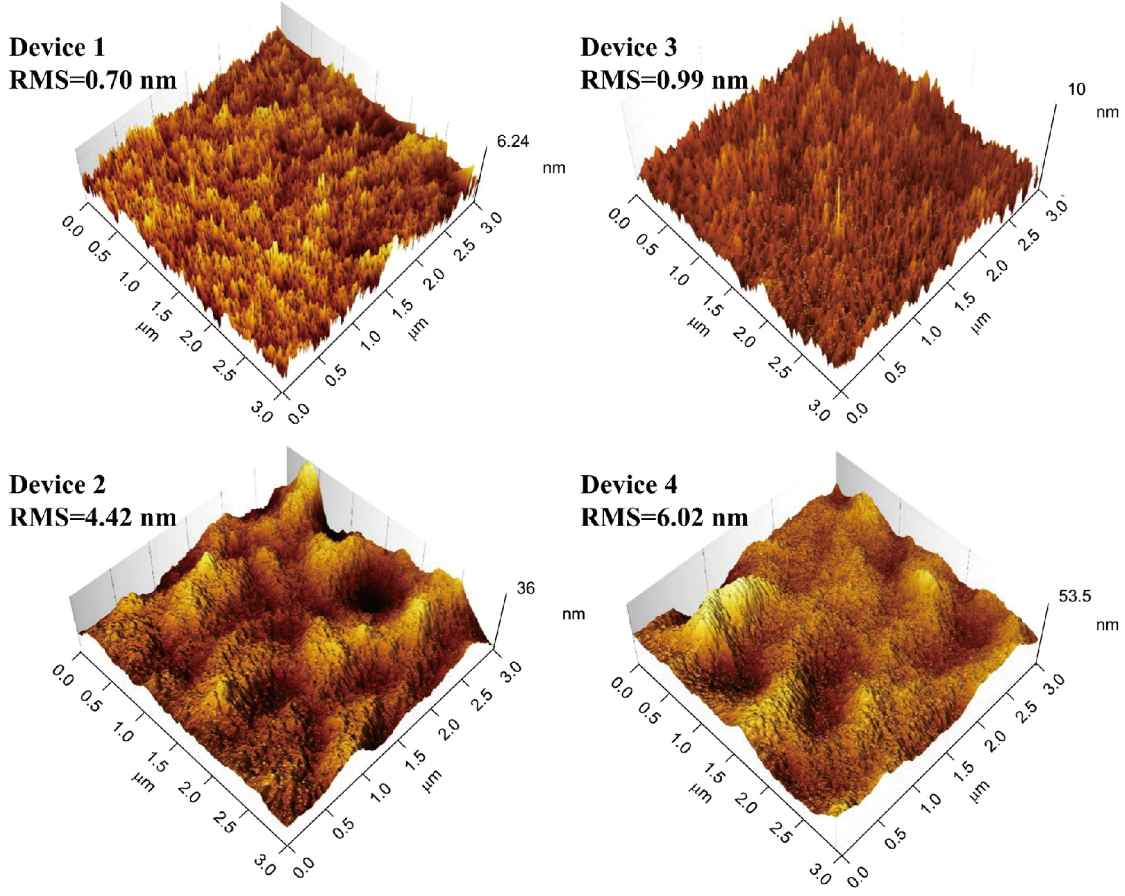

Figure 3 Three dimensional (3D) AFM images of P3HT:$PC_{61}BM$ photoactive layers with different preparation conditions depicted in Table 1.

Table 2 Averaged photovoltaic properties of P3HT:$PC_{61}BM$ BHJ devices based on different fabrication processes

Samples	J_{sc} (mA cm^{-2})	V_{oc} (mV)	FF (%)	PCE (%)
Device 1	5.16±0.19	647±2	54.5±0.1	1.82±0.06
Device 2	10.03±0.23	598±4	61.3±0.4	3.67±0.08
Device 3	6.10±0.21	633±0	58.6±0.5	2.26±0.09
Device 4	10.71±0.25	596±1	61.6±0.4	3.93±0.10

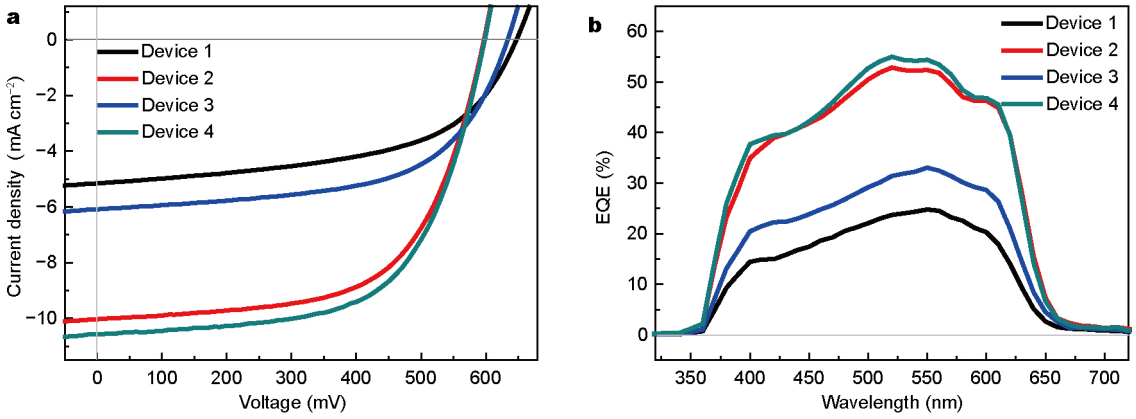

Figure 4 (a) Averaged *J-V* curves of the P3HT:$PC_{61}BM$ devices based on varied dissolution process and SVA post-treatment under the illumination of AM 1.5 G (100 mW cm^{-2}); (b) EQE spectra of the corresponding devices.

and Device 4 are 25%, 52%, 32%, and 56%, respectively, which indicates that charge generation of the devices can be optimized by both approaches.

Time-resolved photoluminescence of P3HT:$PC_{61}BM$ photoactive layer

To examine the effect of processing methods on exciton dissociation process of P3HT:$PC_{61}BM$ films, we measured TRPL kinetics of P3HT:$PC_{61}BM$ blend films with various process methods. As shown in Fig. 5, the PL decays similarly with and without SVA for the photoactive layers treated by the single dissolution process, suggesting that SVA has little influence on exciton dissociation processes for single dissolution processed samples. For the two-step processed samples, the PL decays a bit slower after SVA. The slower decay can be attributed to a phase separation after SVA, which can induce a larger P3HT size and extend exciton diffusion time [12]. For P3HT/$PC_{61}BM$ systems, a suitable phase separation is helpful for improving carrier transport and reducing carrier recombination [12,13,37]. More interestingly, we found that the PL kinetics of two-step processed samples decay faster than those of single dissolution processed samples after SVA, which indicates that the exciton dissociation efficiency is increased by using two-step process method.

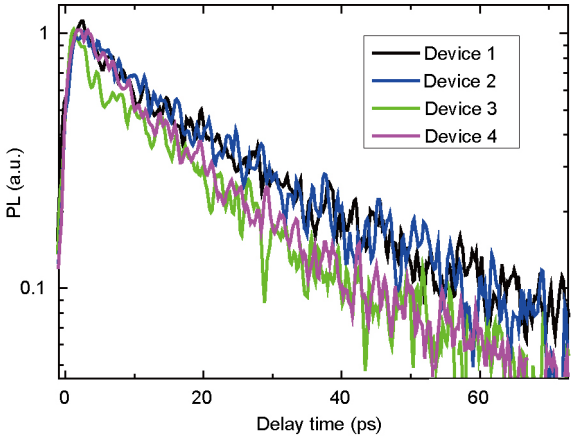

Figure 5 TRPL kinetics of the P3HT:$PC_{61}BM$ films based on different fabrication processes. The excitation and probe wavelengths are 400 and 710 nm, respectively.

Photovoltaic behaviors of PTB7:$PC_{71}BM$ devices

To further verify the enhancement of device efficiency by two-step dissolution processing in PSCs, we also conducted analogues experiments using a PTB7:$PC_{71}BM$ photovoltaic system. Herein, two BHJ PTB7:$PC_{71}BM$ solar cells were fabricated using the single dissolution process (Device 5 and the two-step dissolution process (Device 6). The resulting *J-V* characteristics and photovoltaic parameters are

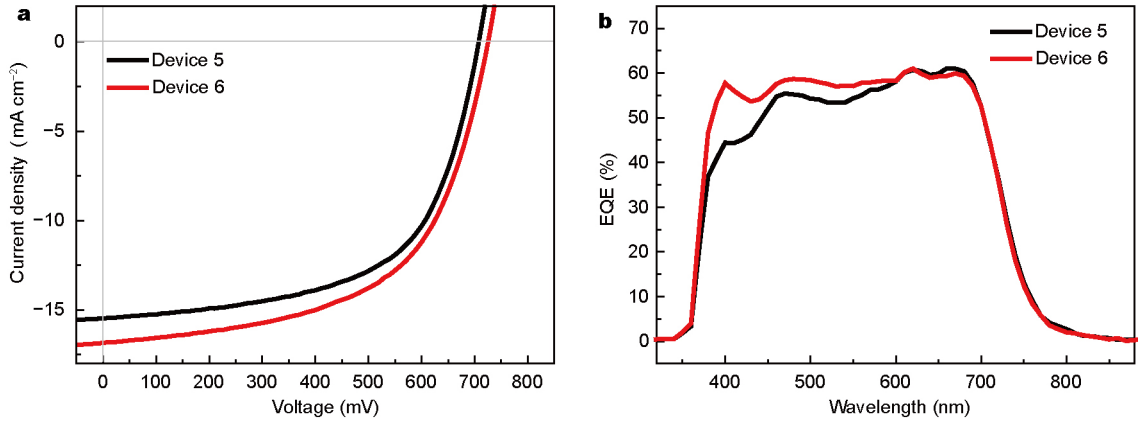

Figure 6 (a) Averaged *J*-*V* curves of the PTB7:$PC_{71}BM$ devices based on varied dissolution process under the illumination of AM 1.5 G (100 mW cm^{-2}); (b) EQE spectra of the corresponding devices.

Table 3 Averaged photovoltaic properties of the PTB7:$PC_{71}BM$ BHJ devices based on different fabrication processes

Samples	J_{sc} (mA cm^{-2})	V_{oc} (mV)	FF (%)	PCE (%)
Device 5	15.59±0.10	708±1	59.4±0.7	6.55±0.03
Device 6	16.85±0.07	725±1	57.8±0.2	7.06±0.05

shown in Fig. 6a and Table 3, respectively. The J_{sc}, V_{oc}, FF, and PCE of Device 5 are 15.59 mA cm^{-2}, 708 mV, 59.4%, and 6.55%, respectively, while for Device 6, the J_{sc} and V_{oc} are raised to 16.85 mA cm^{-2} and 725 mV, with a resulting PCE of 7.06%. We note that the V_{oc} value of the PSC with two-step dissolution processed device was increased from 707 to 725 mV, which is opposite to that of P3HT:$PC_{61}BM$ devices. Generally speaking, V_{oc} in OPVs is determined by the quasi-Fermi level between donors and acceptors which is greatly dominated by the interfacial recombination process. Since we have observed the change of morphology of blend films with and without two-step dissolution process, we speculate the change of V_{oc} may relate to the morphology change which modify the interfacial geometry between donors and acceptors, which has been reported in many references [35,36,38,39]. In addition, as shown in Fig. 6b, the EQE measurement demonstrates that the charge generation of Device 6 is improved compared with that of Device 5, especially within the range of 350–550 nm, corresponding to the absorption of $PC_{71}BM$ [40].

Dissolution and film-forming processes of polymer:fullerene

Based on the above discussions, we propose a model to explain the effect of two-step dissolution on the active layer formation process, as shown in Fig. 7. Before dissolution, the polymer and fullerene are separated. After single dissolution, the polymer and fullerene are evenly distributed in the solvent. Only some polymers, however, are unfolded and kinked polymer chains remain in solution, which has been observed in PBDTTT systems [28,29]. The unfolded polymer configuration will remain in polymer:fullerene films after solvent volatilization. Moreover, it has been found that the ratio of kinked conformation depends on the solvents [28,29]. When the polymer:fullerene film is redissolved in another solvent, the configuration of original kinked polymers can be further extended to the unfolded mode by solvent-induced regulation. The unfolded polymer configuration can then be maximally preserved after the two-step dissolution. As a consequence, the unfolded structure can be easily formulated by the post-processing steps to achieve ordered P3HT structures, which can improve the performance of PSCs.

CONCLUSION

In conclusion, we investigated the effect of the dissolution process of polymer:fullerene on the morphology of thephotoactive layer and device performance. The results reveal that the morphology of the photoactive layer and device performance can be optimized via the two-step dissolution process. According to the *J*-*V* measurements, the J_{sc} is the most sensitive device parameter which is related to the structure of the photoactive layer and exciton dissociation efficiency. In addition, we propose a model to explain the film-forming processes of photoactive blends based on this dissolution process method, and the core idea of the model is that the polymer conformation can be regulated

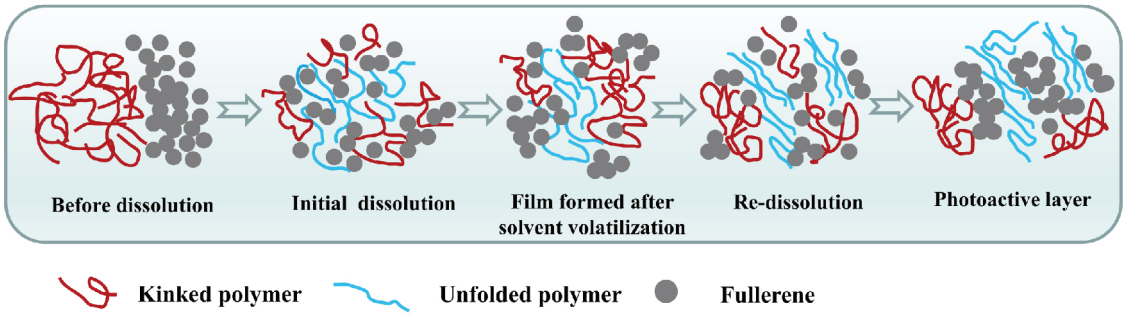

Figure 7 The formation process of polymer:fullerene BHJ photoactive layer via re-dissolution treatment.

by the two-step dissolution process. Thus, we consider the two-step dissolution process to have important reference value for the fabrication of PSCs.

Received 14 September 2016; accepted 12 October 2016; published online 19 October 2016

1 Leonat L, White MS, Głowacki ED, *et al.* 4% Efficient polymer solar cells on paper substrates. J Phys Chem C, 2014, 118: 16813–16817
2 Tipnis R, Bernkopf J, Jia S, *et al.* Large-area organic photovoltaic module—fabrication and performance. Solar Energy Mater Solar Cells, 2009, 93: 442–446
3 Wang JC, Weng WT, Tsai MY, *et al.* Highly efficient flexible inverted organic solar cells using atomic layer deposited ZnO as electron selective layer. J Mater Chem, 2010, 20: 862–866
4 Gaudiana R. Third-generation photovoltaic technology–the potential for low-cost solar energy conversion. J Phys Chem Lett, 2010, 1: 1288–1289
5 Chen JD, Cui C, Li YQ, *et al.* Single-junction polymer solar cells exceeding 10% power conversion efficiency. Adv Mater, 2015, 27: 1035–1041
6 Chen CC, Chang WH, Yoshimura K, *et al.* An efficient triple-junction polymer solar cell having a power conversion efficiency exceeding 11%. Adv Mater, 2014, 26: 5670–5677
7 Huang J, Li CZ, Chueh CC, *et al.* 10.4% power conversion efficiency of ITO-free organic photovoltaics through enhanced light trapping configuration. Adv Energy Mater, 2015, 5: 1500406
8 Zhang S, Ye L, Zhao W, *et al.* Realizing over 10% efficiency in polymer solar cell by device optimization. Sci China Chem, 2015, 58: 248–256
9 Yao H, Ye L, Fan B, *et al.* Influence of the alkyl substitution position on photovoltaic properties of 2D-BDT-based conjugated polymers. Sci China Mater, 2015, 58: 213–222
10 Po R, Maggini M, Camaioni N. Polymer solar cells: recent approaches and achievements. J Phys Chem C, 2010, 114: 695–706
11 Lu L, Yu L. Understanding low bandgap polymer PTB7 and optimizing polymer solar cells based on it. Adv Mater, 2014, 26: 4413–4430
12 Zhang W, Hu R, Li D, *et al.* Primary dynamics of exciton and charge photogeneration in solvent vapor annealed P3HT/PCBM films. J Phys Chem C, 2012, 116: 4298–4310
13 Hu R, Zhang W, Fu LM, *et al.* Spectroelectrochemical characterization of anionic and cationic polarons in poly(3-hexylthiophene)/fullerene blend. Effects of morphology and interface. Synth Met, 2013, 169: 41–47
14 Clarke TM, Durrant JR. Charge photogeneration in organic solar cells. Chem Rev, 2010, 110: 6736–6767
15 Guo F, Kubis P, Li N, *et al.* Solution-processed parallel tandem polymer solar cells using silver nanowires as intermediate electrode. ACS Nano, 2014, 8: 12632–12640
16 Yim JH, Joe S, Pang C, *et al.* Fully solution-processed semitransparent organic solar cells with a silver nanowire cathode and a conducting polymer anode. ACS Nano, 2014, 8: 2857–2863
17 Son SK, Kim YS, Son HJ, *et al.* Correlation between polymer structure and polymer:fullerene blend morphology and its implications for high performance polymer solar cells. J Phys Chem C, 2014, 118: 2237–2244
18 Constantinou I, Lai TH, Klump ED, *et al.* Effect of polymer side chains on charge generation and disorder in PBDTTPD solar cells. ACS Appl Mater Interfaces, 2015, 7: 26999–27005
19 Li G, Shrotriya V, Huang J, *et al.* High-efficiency solution processable polymer photovoltaic cells by self-organization of polymer blends. Nat Mater, 2005, 4: 864–868
20 Chang JF, Sun B, Breiby DW, *et al.* Enhanced mobility of poly(3-hexylthiophene) transistors by spin-coating from high-boiling-point solvents. Chem Mater, 2004, 16: 4772–4776
21 Yao Y, Hou J, Xu Z, *et al.* Effects of solvent mixtures on the nanoscale phase separation in polymer solar cells. Adv Funct Mater, 2008, 18: 1783–1789
22 Zhang F, Jespersen KG, Björström C, *et al.* Influence of solvent mixing on the morphology and performance of solar cells based on polyfluorene copolymer/fullerene blends. Adv Funct Mater, 2006, 16: 667–674
23 Ye L, Zhang S, Ma W, *et al.* From binary to ternary solvent: morphology fine-tuning of D/A blends in PDPP3T-based polymer solar cells. Adv Mater, 2012, 24: 6335–6341
24 Agostinelli T, Ferenczi TAM, Pires E, *et al.* The role of alkane dithiols in controlling polymer crystallization in small band gap polymer:fullerene solar cells. J Polym Sci B Polym Phys, 2011, 49: 1345–1345
25 McDonald SA, Konstantatos G, Zhang S, *et al.* Solution-processed PbS quantum dot infrared photodetectors and photovoltaics. Nat Mater, 2005, 4: 138–142
26 Huang PT, Chang YS, Chou CW. Preparation of porous poly(3-hexylthiophene) by freeze-dry method and its application to organic photovoltaics. J Appl Polym Sci, 2011, 122: 233–240
27 Li L, Lu G, Yang X. Improving performance of polymer photovoltaic devices using an annealing-free approach via construction of ordered aggregates in solution. J Mater Chem, 2008, 18: 1984–1990
28 Huo MM, Liang R, Xing YD, *et al.* Side-chain effects on the solution-phase conformations and charge photogeneration dynamics of low-bandgap copolymers. J Chem Phys, 2013, 139: 124904–124904

29 Huo MM, Hu R, Xing YD, *et al.* Impacts of side chain and excess energy on the charge photogeneration dynamics of low-bandgap copolymer-fullerene blends. J Chem Phys, 2014, 140: 084903
30 Zhao NJ, Lin ZH, Zhang W, *et al.* Charge photogeneration dynamics of poly(3-hexylthiophene) blend with covalently-linked fullerene derivative in low fraction. J Phys Chem C, 2014, 118: 21377–21384
31 Spano FC. Modeling disorder in polymer aggregates: the optical spectroscopy of regioregular poly(3-hexylthiophene) thin films. J Chem Phys, 2005, 122: 234701–234701
32 Chien CH, Kung LR, Wu CH, *et al.* A solution-processable bipolar molecular glass as a host material for white electrophosphorescent devices. J Mater Chem, 2008, 18: 3461–3466
33 Li D, Liang R, Yue H, Wang P, Fu LM, Zhang JP, Ai XC. Influence of donor and acceptor mass ratios on P3HT:PCBM film structure and device performance. Acta Phys-Chim Sin, 2012, 28: 1373–1379
34 Shrotriya V, Yao Y, Li G, *et al.* Effect of self-organization in polymer/fullerene bulk heterojunctions on solar cell performance. Appl Phys Lett, 2006, 89: 063505
35 Scharber MC, Mühlbacher D, Koppe M, *et al.* Design rules for donors in bulk-heterojunction solar cells—towards 10% energy-conversion efficiency. Adv Mater, 2006, 18: 789–794
36 Tsoi WC, Spencer SJ, Yang L, *et al.* Effect of crystallization on the electronic energy levels and thin film morphology of P3HT:PCBM blends. Macromolecules, 2011, 44: 2944–2952
37 Guo J, Ohkita H, Yokoya S, *et al.* Bimodal polarons and hole transport in poly(3-hexylthiophene):fullerene blend films. J Am Chem Soc, 2010, 132: 9631–9637
38 Ohzeki M, Fujii S, Arai Y, *et al.* Performance improvement of flexible bulk heterojunction solar cells using PTB7:PC_{71} BM by optimizing spin coating and drying processes. Jpn J Appl Phys, 2014, 53: 02BE04
39 Guo S, Ning J, Körstgens V, *et al.* The effect of fluorination in manipulating the nanomorphology in PTB7:PC_{71} BM bulk heterojunction systems. Adv Energy Mater, 2015, 5: 1401315
40 Yang T, Wang M, Duan C, *et al.* Inverted polymer solar cells with 8.4% efficiency by conjugated polyelectrolyte. Energy Environ Sci, 2012, 5: 8208–8214

Acknowledgments The work was supported by the National Natural Science Foundation of China (21603020, 61505018 and 51503022), the Scientific and Technological Research Program of Chongqing Municipal Education Commission (KJ1501116 and KJ1401122), the Basic and Frontier Research Program of Chongqing Municipality (cstc2016jcyjA0451, cstc2015jcyjA90020 and cstc2016jcyjA0140), and the Introduction of Talent Projects of Chongqing University of Arts and Sciences (R2014CJ05 and R2012CH09). The study was also supported by NPRP grant #NPRP7-227-1-034 from Qatar National Research Fund.

Author contributions Zhang W, Zheng K and Guo C designed and directed the research. Hu R and Cheng J fabricated and characterized the polymer thin films and devices. Zhang W conducted TRPL measurement of the blend films. Ni H, Liu H and Zhu J conducted UV and AFM experiments. Liu Y and Li L provided polymer and PCBM materials. All authors contributed to discuss the results. Zhang W and Zheng K wrote the manuscript with inputs from all authors.

Conflict of interest The authors declare that there is no conflict of interests.

Supplementary information Supplementary information is available in the online version of this article.

Rong Hu received his PhD degree from Renmin University of China in 2014. He is a lecturer at the Research Institute for New Materials Technology of Chongqing University of Arts and Science. His current research interests are the fabrication of organic photovoltaic devices.

Jiang Cheng received his PhD degree from Sichuan University in 2012. He is a lecturer at the Research Institute for New Materials Technology of Chongqing University of Arts and Science. His current research interests are earth abundant photovoltaic materials and organic photovoltaic devices.

Wei Zhang received his PhD degree in optics from the Department of Physics, Harbin Institute of Technology in 2013. He is currently a postdoctoral researcher at the Division of Chemical Physics, Lund University. His research interest includes charge photogeneration and recombination process in polymer solar cells and group III-V nanowires.

Chaozhong Guo received his PhD degree at Chongqing University in 2013. He is an associate professor of chemical engineering and top-notch talent at Chongqing University. His research focuses on green synthesis of graphdiyne-based nanomaterials, including composites derived from conductive nanopolymers and applications in energy conversion and storage.

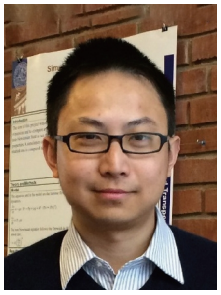

Kaibo Zheng received his PhD degree from the Department of Material Science, Fudan University in 2010. He is now a senior researcher at the Department of Chemical Physics at Lund University, Sweden. His research interests include design, structural characterization, and ultrafast photo-induced dynamics of nanostructured optoelectronic materials such as semiconductor quantum dots, nanowires, and perovskite materials.

提高聚合物太阳电池性能的新方法: 两步溶解法制备电池活性层

胡荣[1†], 程江[1†], 倪海涛[1], 朱江[1], 柳红东[1], 张伟[2*], 刘玉荣[1], 李璐[1], 郭朝中[1*], 郑凯波[2,3*]

摘要 本文以P3HT:$PC_{61}BM$和PTB7:$PC_{71}BM$两种有机光伏体系为研究对象, 探讨了光伏材料的“两步”溶解处理对聚合物太阳电池性能的影响. P3HT:$PC_{61}BM$光活性层的光学与形貌表征揭示了P3HT的有序相结构和给/受体相分离结构可以被“两步”溶解处理进一步优化; 瞬态荧光数据表明, P3HT:$PC_{61}BM$光活性材料经“两步”溶解处理后, 激子的分离能力得到增强. 经“两步”溶解处理后的器件性能较“一步”溶解处理的器件性能提高了24%. 此外, 同样的处理方式应用于PTB7:$PC_{71}BM$体系, 可使器件的光伏性能提高8%. 因此, 光活性材料的“两步”溶解处理是一种简单、有效的提高聚合物光伏性能的优化方法.